Journal of Sound and Vibration (2002) **249**(5), 939–954
doi:10.1006/jsvi.2001.3881, available online at http://www.idealibrary.com on IDEAL®

WAVENUMBER PREDICTION OF WAVES IN BURIED PIPES FOR WATER LEAK DETECTION

J. M. Muggleton, M. J. Brennan and R. J. Pinnington

Institute of Sound and Vibration Research, Southampton University, Highfield, Southampton SO17 1BJ, England

(*Received* 31 *January* 2001, *and in final form* 2 *July* 2001)

Water leaks are a topic of great concern in Britain and many other countries, because of decreasing water supplies and the deterioration of old pipework. Correlation techniques are widely used in leak detection, but for these to be effective, the propagation wavespeeds and wave attenuation must be known. Relatively predictable for metal pipes, these are largely unknown for the newer plastic pipes, being highly dependent on the pipe wall properties and the surrounding medium. In this paper, pipe equations for $n = 0$ axisymmetric wave motion are derived for a fluid-filled pipe, surrounded by an infinite elastic medium which can support both longitudinal and shear waves. These equations are solved for two wave types, $s = 1, 2$, which correspond to a fluid dominated wave and an axial shell wave, and expressions for a complex wavenumber for each wave are given.

1. INTRODUCTION

Water leakage from buried pipes is a subject of great concern in Britain, and across the world because of decreasing water supplies due to changing rainfall patterns, deterioration or damage to the distribution system, and an ever increasing population. A significant amount of water can be lost due to leakage, and over the past few years much attention has been focused on trying to reduce this wastage of resources.

For many years, the most useful technique for locating a leak has been the correlation of leak noise at two locations along the pipe [1]. The leak position is identified by the delay between the leak noise reaching each monitoring point. Although the current acoustic technique enjoys some success when employed on metal pipework, there are significant problems in locating leaks when the pipework is plastic, the technique in this situation not being well established [2]. For the correlation technique to be effective, the propagation wavespeeds and wave attenuation must be known *a priori*. Relatively predictable for metal pipes, there is considerably more uncertainty with plastic pipes, as the wave propagation behaviour becomes highly coupled between the pipe wall and the contained fluid and surrounding medium [3, 4]. Consequently, the wavespeeds and losses in water pipes are highly dependent on the pipe wall properties and the surrounding medium.

The problem of vibration and wave propagation within elastic, fluid-filled pipes has been studied previously in some detail, see for example references [5–7], and physical interpretations of the results have been offered. Similarly, the radiation from submerged, empty cylinders has been well documented, see for example references [4, 8]. However, when the pipe both contains fluid and is surrounded by some medium, little work is available in the literature, although some work primarily aimed at high frequencies has recently been carried out [9, 10].

0022-460X/02/050939 + 16 $35.00/0

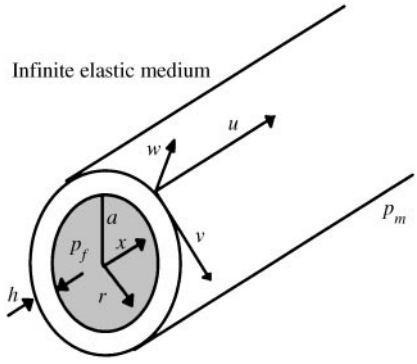

Figure 1. The co-ordinate system for a fluid-filled pipe surrounded by an infinite elastic medium.

Observing common practice within the leak detection community reveals that leak detection is most successfully executed on low-frequency signals, suggesting that these frequencies are both excited by the leak and propagate most effectively. In addition, recent work in Canada on a plastic distribution system [2] has confirmed that most leak noise energy, on simulated but realistic leaks, is concentrated at frequencies below 100 Hz.

The focus of this work, therefore is on the low-frequency behaviour of fluid-filled pipes surrounded by another elastic medium. Well below the pipe ring frequency, four wave types are responsible for most of the energy transfer [5, 6]: three axisymmetric waves ($n = 0$) and the $n = 1$ wave, related to beam bending. Of the $n = 0$ waves, the first, termed $s = 1$, is a predominantly fluid-borne wave; the second wave, $s = 2$, is predominantly a compressional wave in the shell; the third wave, $s = 0$, is a torsional wave uncoupled from the fluid. This work develops on previous work [5], in which wavenumbers were derived for the $s = 1$ and 2 axisymmetric wave types for a fluid-filled elastic pipe *in vacuo*; the work is extended here to consider the case of a buried pipe. Expressions for the wavenumbers are derived, and the effects of the surrounding medium are investigated.

2. THE EQUATIONS OF MOTION

The pipe equations for $n = 0$ axisymmetric wave motion are derived for a fluid-filled pipe, surrounded by an infinite elastic medium which can sustain both longitudinal and shear waves. These equations are solved for two wave types, $s = 1, 2$, which correspond to a fluid dominated wave and an axial shell dominated wave. Both of these wave types involve motion of the shell and the fluid. Solutions are expressed in terms of a complex wavenumber for each wave, the real part of which gives the wavespeed, and the imaginary part of which gives the wave attenuation.

With reference to Figure 1, the shell displacements are u, v and w in the axial (x), circumferential (θ), and radial (r) directions respectively. The following are simplified forms of Kennard's equations for a thin-walled shell [11], with shell bending neglected, and so are only valid below the ring frequency.

Equilibrium of forces in the axial direction gives

$$\rho\ddot{u} = \partial\sigma_x/\partial x. \tag{1}$$

Equilibrium of forces in the radial direction, upon assuming no circumferential variation, leads to

$$(p_f(a) - p_m(a))(a/h) = \sigma_\theta + \rho a\ddot{w}, \tag{2}$$

(note that the pressures are evaluated at $r = a$), where σ_x and σ_θ are the axial and circumferential stresses, respectively, p_f and p_m are the pressures in the internal and external media, respectively; ρ is the density of the shell material; and a and h are the radius and thickness of the shell wall respectively ($h \ll a$). Hooke's Law relationships for the shell are

$$\sigma_\theta = \frac{E}{1-\nu^2}\left(\frac{w}{a} + \nu\frac{\partial u}{\partial x}\right), \quad \sigma_x = \frac{E}{1-\nu^2}\left(\frac{\partial u}{\partial x} + \nu\frac{w}{a}\right). \tag{3, 4}$$

E and ν are the shell material Young's modulus and the Poisson ratio, respectively; w/a and $\partial u/\partial x$ are the circumferential and axial strains respectively.

Equations (1) and (4) may be combined to give

$$\rho\ddot{u} - \frac{E}{1-\nu^2}\left(\frac{\partial^2 u}{\partial x^2} + \frac{\nu}{a}\frac{\partial w}{\partial x}\right) = 0. \tag{5}$$

Equations (2) and (3) yield

$$\rho a\ddot{w} + \frac{E}{1-\nu^2}\left(\frac{w}{a} + \nu\frac{\partial u}{\partial x}\right) = [p_f(a) - p_m(a)]\frac{a}{h}. \tag{6}$$

These are the two coupled shell equations for $n = 0$ motion.

Travelling wave solutions of the form

$$u = \sum_{s=1}^{2} U_s e^{i(\omega t - k_s x)}, \qquad w = \sum_{s=1}^{2} W_s e^{i(\omega t - k_s x)} \tag{7, 8}$$

may be used to describe the displacements, where ω is the angular frequency and k_s is the axial wavenumber for the s wave.

Upon assuming that the internal medium is a fluid, which cannot sustain shear, the internal pressure p_f can be described by a Bessel function of order zero,

$$p_f = \sum_{s=1}^{2} P_{fs} J_0(k_{fs}^r r) e^{i(\omega t - k_s x)}, \tag{9}$$

where the internal radial wavenumber, k_{fs}^r, is related to the fluid wavenumber, k_f, by

$$(k_{fs}^r)^2 = k_f^2 - k_s^2. \tag{10}$$

The pressure in the external medium, p_m, can be described by the sum of two Hankel functions of order zero,[†] one corresponding to an outgoing longitudinal wave, and one corresponding to an outgoing shear wave. No incoming waves are present as the medium is considered to be of infinite extent,

$$p_m = \sum_{s=1}^{2} P_{ds} H_0(k_{ds}^r r) e^{i(\omega t - k_s x)} + \sum_{s=1}^{2} P_{rs} H_0(k_{rs}^r r) e^{i(\omega t - k_s x)}, \tag{11}$$

[†]Upon adopting the $e^{i\omega x}$ time dependence convention, the Hankel functions which describe outgoing waves are Hankel functions of the second kind.

where the subscripts d and r refer to the longitudinal (*d*ilatational) and shear (*r*otational) wave types respectively. The radial components of the longitudinal and shear wavenumbers are given by

$$(k^r_{ds})^2 = k_d^2 - k_s^2, \qquad (k^r_{rs})^2 = k_r^2 - k_s^2. \tag{12, 13}$$

k_d and k_r are the longitudinal and shear wavenumbers, respectively, in the external medium. Substitution of these pressure and displacement solutions into equations (5) and (6) gives the following relationships for the s wavenumbers:

$$(k_L^2 a^2 - k_s^2 a^2) U_s = \mathrm{i}\nu k_s a W_s, \tag{14}$$

$$W_s(1 - k_L^2 a^2) - \mathrm{i}\nu k_s a U_s = [P_{fs} \mathrm{J}_0(k^r_{fs} a) - P_{ds} \mathrm{H}_0(k^r_{ds} a) - P_{rs} \mathrm{H}_0(k^r_{rs} a)] \frac{a^2(1-\nu^2)}{Eh}, \tag{15}$$

where k_L is the wavenumber of a compressional wave in a plate, given by $k_L^2 = \omega^2 \rho(1-\nu^2)/E$.

Each of the pressure waves, $s = 1, 2$, must have a radial displacement at the boundary $r = a$ which is equal to the shell displacement. Equating the radial velocity of the fluid at the shell wall (both internally and externally) to the radial velocity of the shell wall gives independent expressions for the pressure coefficients P_{fs}, P_{ds} and P_{rs}:

$$P_{fs} = \omega^2 \rho_f \, W_s / k^r_{fs} \mathrm{J}'_0(k^r_{fs} a) \tag{16}$$

$$P_{ds} = \omega^2 \rho_m \frac{W_s}{k^r_{ds} \mathrm{H}'_0(k^r_{ds} a)}, \qquad P_{rs} = \omega^2 \rho_m \frac{W_s}{k^r_{rs} \mathrm{H}'_0(k^r_{rs} a)} \tag{17, 18}$$

where ρ_f and ρ_m are the internal and external medium densities, respectively, and the prime denotes differentiation with respect to the argument.

Substituting equations (14) and (16)–(18) into equation (15) gives

$$1 - k_L^2 a^2 + \nu^2 \frac{k_s^2}{k_L^2 - k_s^2} = \frac{B_f a(1-\nu^2)}{Eh} \frac{k_f^2 a^2}{k^r_{fs} a} \frac{\mathrm{J}_0(k^r_{fs} a)}{\mathrm{J}'_0(k^r_{fs} a)} - \frac{B_m a(1-\nu^2)}{Eh} \frac{k_d^2 a^2}{k^r_{ds} a} \frac{\mathrm{H}_0(k^r_{ds} a)}{\mathrm{H}'_0(k^r_{ds} a)}$$
$$- \frac{G_m a(1-\nu^2)}{Eh} \frac{k_r^2 a^2}{k^r_{rs} a} \frac{\mathrm{H}_0(k^r_{rs} a)}{\mathrm{H}'_0(k^r_{rs} a)}. \tag{19}$$

B_f and B_m are the bulk moduli of the internal and external media, respectively, and G_m is the shear modulus of external medium.

Equation (19) may be re-expressed in terms of the impedances of the longitudinal and shear waves in the external medium, z_{ds} and z_{rs}. In addition, for small arguments, when there is less than one half of a fluid wavelength across the pipe diameter, the small argument approximations for the Bessel functions may be used [12]. Equation (19) then becomes

$$1 - k_L^2 a^2 + \nu^2 \frac{k_s^2}{k_L^2 - k_s^2} = -\frac{2B_f a(1-\nu^2)}{Eh} \frac{k_f^2}{k_f^2 - k_s^2} - \mathrm{i}\omega \frac{a^2(1-\nu^2)}{Eh} z_{ds} - \mathrm{i}\omega \frac{a^2(1-\nu^2)}{Eh} z_{rs}, \tag{20}$$

where

$$z_{ds} = \frac{-\mathrm{i}\rho_m c_d k_d}{k^r_{ds}} \frac{\mathrm{H}_0(k^r_{ds} a)}{\mathrm{H}'_0(k^r_{ds} a)} \quad \text{and} \quad z_{rs} = \frac{-\mathrm{i}\rho_m c_r k_r}{k^r_{rs}} \frac{\mathrm{H}_0(k^r_{rs} a)}{\mathrm{H}'_0(k^r_{rs} a)}. \tag{21}$$

c_d and c_r are the wavespeeds of the longitudinal and shear waves respectively.

2.1. WAVE IMPEDANCES IN THE SURROUNDING MEDIUM

Equation (21) gives the form of the impedances for the outgoing waves in the surrounding medium. Each impedance is a function of both the wavenumber in the external medium, and the radial component of that wavenumber: i.e., the impedance is a function of both frequency and wave angle.

When the argument of the Hankel functions (the radial wavenumber) has a non-zero real component (i.e., is either purely real or is complex), the Hankel function ratios are complex, resulting in a radiation impedance which has both real and imaginary components; when the radial wavenumber is purely imaginary, the Hankel function ratios are purely real, resulting in a radiation impedance which is purely imaginary: i.e., purely reactive.

Equations (12) and (13) show that, for real k_d, k_r and k_s, the radial wavenumber is real, and thus the resulting impedance complex, provided that the respective wavenumbers of the waves in the surrounding medium are greater than the wavenumber of the s wave in the pipe: i.e., when the wavespeed of the s wave in the pipe is greater than the wavespeed of the respective wave in the surrounding medium. When the wavespeed of the s wave in the pipe is less than the wavespeed of a wave in the surrounding medium, the resulting wave impedance is purely imaginary. When the wavenumbers k_d, k_r and k_s are complex, such as when the s wave decays as it propagates or when the contained medium or pipe wall material are allowed to be lossy, the wave impedances are always complex. Under these circumstances, for the longitudinal wave, for example, the wave impedance is predominantly reactive (i.e., has only a small real component) when $\mathrm{Re}\{k_d^2\} \geqslant \mathrm{Re}\{k_s^2\}$, and has a significant resistive (real) component when $\mathrm{Re}\{k_d^2\} \leqslant \mathrm{Re}\{k_s^2\}$ [13]. Similar reasoning may be applied to the shear wave. Junger and Feit [4] have given low-frequency approximations to the wave impedances z_{ds} and z_{rs}, which are valid provided that the radial wavenumbers are small enough such that $|k_{ds}^r a| \ll 1$ and $|k_{rs}^r a| \ll 1$. When the impedance is purely reactive, it is mass-like although the mass itself is frequency dependent: i.e.,

$$z_{ds} = \mathrm{i}\omega m_{ds}, \tag{22}$$

where $m_{ds} \approx -\rho_m a \ln(|k_{ds}^r a|)$
z_{rs} has a similar form. When the impedance has resistive and reactive components it becomes

$$z_{ds} \approx (\rho_m a \pi/2)\,\omega + \mathrm{i}\omega m_{ds}, \tag{23}$$

where m_{ds} is defined as above. Again, z_{rs} is of a similar form.

Figure 2 shows the form of the radiation impedance for different ratios of axial wavenumber to wavenumber, k in the external medium ($k = k_d$ or $k = k_m$, depending on which wave is being considered). The above low-frequency approximations are also shown. Figures 2(a) and 2(b) show the real and imaginary components of the radiation impedance for various values of $k_s/k < 1$ (i.e., when the axial wavespeed in the pipe is greater than the wavespeed in the surrounding medium, and the wave is radiating into the surrounding medium). When $k_s/k = 0$, the axial wavespeed is infinite, and the pipe behaves as a pulsating cylinder, with the waves radiating out radially, and the real part of the impedance tending to unity at high frequencies as expected. For increasing values of the ratio k_s/k, the propagating wave in the surrounding medium becomes more and more aligned with the pipe axis, and both the real and imaginary components of the radiation impedance increase. For the limiting case of $k_s = k$, the wave is propagating parallel to the pipe axis; the low-frequency approximation for the radiation resistance becomes exact at all frequencies,

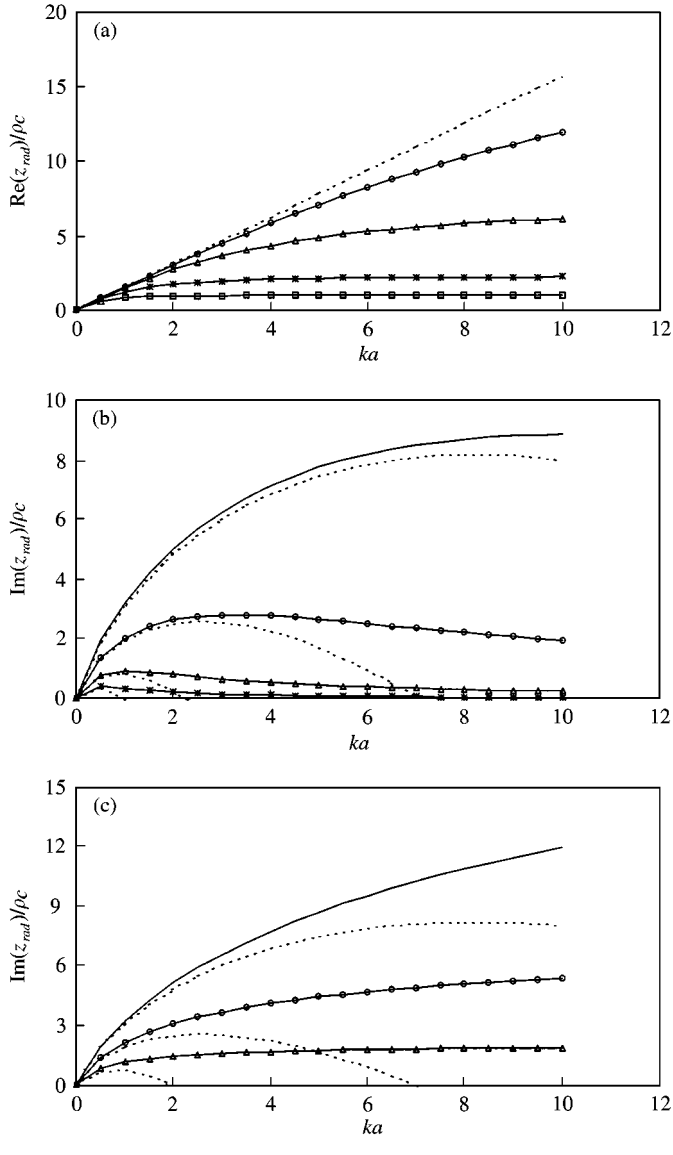

Figure 2. Normalized radiation impedance as a function of non-dimensional freefield wavenumber, k, in the surrounding medium, for different values of k_s/k. (a) Real part, $k_s < k$: -----, lim $k_s/k \to 1$; —⊟—, $k_s/k = 0$; —✱—, $k_s/k = 0{\cdot}9$; —△—, $k_s/k = 0{\cdot}99$; —○—, $k_s/k = 0{\cdot}999$. (b) Imaginary part, $k_s < k$: —✱—, $k_s/k = 0$; —△—, $k_s/k = 0{\cdot}9$; —○—, $k_s/k = 0{\cdot}99$; ——, $k_s/k = 0{\cdot}999$. (c) Imaginary part, $k_s > k$: —△—, $k/k_s = 0{\cdot}9$; —○—, $k/k_s = 0{\cdot}99$; ——, $k/k_s = 0{\cdot}999$ (the dotted lines show the low-frequency approximation).

and the radiation reactance becomes infinite. Figure 2(c) shows the imaginary components of the radiation impedance for values of $k_s/k > 1$ (i.e., when the axial wavespeed in the pipe is less than the wavepseed in the surrounding medium, and the wave does not radiate into the surrounding medium). Under these circumstances, the real part of the radiation impedance is zero. With increasing k_s/k, the radiation reactance decreases from infinity, but stays positive, showing that the effect of the surrounding medium is always to mass load the pipe. These effects have been discussed more fully by Junger [9].

3. SOLUTION FOR THE $s = 1$ WAVE

Equation (20) allows the s wavenumbers to be determined.

The $s = 1$ wavenumber (the predominantly fluid-borne wave) is found by assuming that k_1 is much larger than the plate compressional wavenumber k_L: i.e., the wavespeed of the $s = 1$ wave is much slower than the plate compressional wavespeed. Setting $k_1^2 \gg k_L^2$ gives

$$1 - k_L^2 a^2 - v^2 = -\frac{2B_f a(1-v^2)}{Eh}\frac{k_f^2}{k_f^2 - k_1^2} - \mathrm{i}\omega\frac{a^2(1-v^2)}{Eh}z_{d1} - \mathrm{i}\omega\frac{a^2(1-v^2)}{Eh}z_{r1}, \quad (24)$$

which, on rearranging, and adopting the form of the low-frequency approximations for the impedances of the surrounding medium (equation (23)) becomes

$$k_1^2 = k_f^2\left(1 + \frac{2B_f/a}{(Eh/a^2) - \omega^2(\rho h + M_{rad}) + \mathrm{i}\omega R_{rad}}\right), \quad (25)$$

where $z_{d1} + z_{r1} = R_{rad} + \mathrm{i}\omega M_{rad}$.

Expressing k_1 in this form allows the individual terms to be readily identified as stiffness components of the contained fluid ($2B_f/a$) and the pipe wall (Eh/a^2), a pipe wall mass component ($\rho h\omega^2$), and the radiation mass and resistance of the surrounding medium (M_{rad} and R_{rad}). It should be noted that the impedance terms M_{rad} and R_{rad} are dependent on k_1, which must therefore strictly be found recursively. However, a number of observations may now be made.

(1) If the density of the surrounding medium is sufficiently low, the radiation impedance M_{rad} and R_{rad} will be small compared with the mass term $\rho h\,\omega^2$, and may be ignored. This is then equivalent to the case when no surrounding medium is present. Under these circumstances, k_1 becomes

$$k_1^2 = k_f^2\left(1 + \frac{(2B_f/a)}{(Eh/a^2) - \rho h\omega^2}\right). \quad (26)$$

This is in agreement with earlier work by Pinnington and Briscoe [5] and Munjal and Thawani [7], when considering the case of no surrounding medium. The fluid wave in the pipe is always slower than the fluid wave in an infinite medium, the wavespeed decreasing with increasing frequency. As the frequency approaches the pipe ring frequency, the denominator of equation (26) tends to zero, so the wavenumber k_1 approaches infinity, and the wavespeed correspondingly approaches zero.

(2) At low frequencies (well below the pipe ring frequency), the pipe wall inertia and radiation mass terms will be small compared with the pipe wall stiffness term, Eh/a^2, and equation (25) reduces to the Korteweg equation [14] with an additional loss term R_{rad}, where k_1 depends primarily on the magnitude of the stiffness of the contained fluid compared with that of the pipe wall:

$$k_1^2 = k_f^2\left(1 + \frac{(2B_f/a)}{(Eh/a^2) + \mathrm{i}\omega R_{rad}}\right). \quad (27)$$

(3) Equation (25) may be reformulated in terms of the impedance of the contained fluid, z_{fluid}, the impedance of the pipe wall, z_{pipe}, and the radiation impedance, z_{rad1}, namely

$$k_1^2 = k_f^2\left(1 + \frac{z_{fluid}}{z_{pipe} + z_{rad1}}\right), \quad (28)$$

where $z_{fluid} = -2iB_f/a\omega$, $z_{pipe} = i(\rho h\omega - Eh/a^2\omega)$, and $z_{rad1} = z_{d1} + z_{r1}$. The magnitudes of the individual terms and their variation with frequency are considered in more detail in section 5, where example results are discussed.

(4) Returning to equation (25), whilst the effect of the pipe wall on the $s = 1$ wave in the fluid is to increase the wavenumber k_1 from its freefield value k_f, the effect of the surrounding medium is to increase it yet further. In addition, if the radiation resistance term is non-zero, this introduces an imaginary component into k_1, indicating that the wave decays as it propagates, radiating into the surrounding medium. Furthermore, if the shell material itself is lossy, loss within the pipe wall may be represented by a complex elastic modulus, $E(1 + i\eta)$, where η is the material loss factor; equation (25) then becomes

$$k_1^2 = k_f^2\left(1 + \frac{2B_f/a}{(Eh/a^2) - \omega^2(\rho h + M_{rad}) + i(\omega R_{rad} + \eta Eh/a^2)}\right). \tag{29}$$

The equation clearly shows that, at low frequencies, losses within the pipe wall will dominate the loss; at higher frequencies, if the radiation resistance term is non-zero, the loss due to radiation will dominate.

The above effects are discussed further in section 5 where example results are shown.

4. SOLUTION FOR THE $s = 2$ WAVE

The $s = 2$ wavenumber (corresponding to the shell wave) is found with the knowledge that it is always smaller than the fluid wavenumber k_f, and the wavenumbers in the surrounding medium, k_d and k_r. Setting $k_2^2 \ll k_f^2$, $k_2^2 \ll k_d^2$ and $k_2^2 \ll k_r^2$ gives $k_{f2}^r \approx k_f$, $k_{d2}^r \approx k_d$ and $k_{r2}^r \approx k_r$. Substituting into equation (20) gives

$$1 - k_L^2a^2 + \nu^2\frac{k_2^2}{k_L^2 - k_2^2} = -\frac{2B_fa(1-\nu^2)}{Eh} - i\omega\frac{a^2(1-\nu^2)}{Eh}z_{d2} - i\omega\frac{a^2(1-\nu^2)}{Eh}z_{r2}, \tag{30}$$

which, on rearranging, becomes

$$k_2^2 = k_L^2\left(1 + \frac{\nu^2}{1-\nu^2}\frac{(Eh/a^2)}{(Eh/a^2) + (2B_f/a) - \rho h\omega^2 + i\omega(z_{d2} + z_{r2})}\right). \tag{31}$$

As for the $s = 1$ wave, the individual terms can be readily identified as stiffness components of the contained fluid ($2B_f/a$) and the pipe wall (Eh/a^2), a pipe wall mass component ($\rho h\omega^2$), and the impedances of the waves in the surrounding medium (z_{d2} and z_{r2}). Furthermore, the expression for k_2 is explicit as the radiation impedances depend only on the wavenumbers of the waves in the surrounding medium, namely

$$z_{d2} \approx -i\rho_m c_d\frac{H_0(k_da)}{H_0'(k_da)} \quad \text{and} \quad z_{r2} \approx -i\rho_m c_r\frac{H_0(k_ra)}{H_0'(k_ra)}. \tag{32}$$

The implication here is that k_2 is sufficiently small such that the waves in the external medium are assumed to be propagating normal to the pipe wall at all frequencies. In this way, the angular dependence of the impedance functions is removed, and the radiation impedance approaches that of a pulsating cylinder (see section 2.1 and Figure 2).

Upon adopting the form of the low-frequency approximations for the impedances (equation (23)), equation (31) becomes

$$k_2^2 = k_L^2\left(1 + \frac{\nu^2}{1-\nu^2}\frac{Eh/a^2}{(Eh/a^2) + (2B_f/a) - \omega^2(\rho h + M_{rad}) + \mathrm{i}\omega R_{rad}}\right), \tag{33}$$

where $z_{d2} + z_{r2} = R_{rad} + \mathrm{i}\omega M_{rad}$.

Again a number of observations may be made.

(1) As for the $s = 1$ wave, if the density of the surrounding medium is sufficiently low, the radiation mass term will be small compared with the pipe wall inertia term and can be ignored. In addition, the radiation resistance term can be considered negligible. This is then equivalent to the case of no surrounding medium, and the expression for k_2 becomes

$$k_2^2 = k_L^2\left(1 + \frac{\nu^2}{1-\nu^2}\frac{Eh/a^2}{(Eh/a^2) + (2B_f/a) - \rho h\omega^2}\right). \tag{34}$$

Upon assuming that the fluid and shell material are not lossy, the wave does not decay, and k_2 is purely real. The shell wall experiences the contained fluid as a stiffness, and its effect is to reduce the wavenumber k_2 from the empty pipe case. This is in agreement with work previously undertaken by Pinnington and Briscoe [5].

(2) At low frequencies (again well below the pipe ring frequency), the mass terms will be small compared to the stiffness terms and equation (33) becomes

$$k_2^2 = k_L^2\left(1 + \frac{\nu^2}{1-\nu^2}\frac{Eh/a^2}{(Eh/a^2) + (2B_f/a) + \mathrm{i}\omega R_{rad}}\right). \tag{35}$$

The predominant effect of the external medium here is to introduce an imaginary component to k_2: i.e., the wave decays as it propagates along the shell, but its speed is largely unaffected.

(3) Equation (33) may be reformulated in terms of the impedance of the contained fluid, z_{fluid}, the impedance of the pipe wall, z_{pipe}, the impedance of the pipe wall stiffness, z_{Kpipe}, and the radiation impedance, z_{rad2}, namely

$$k_2^2 = k_L^2\left(1 + \frac{\nu^2}{1-\nu^2}\frac{z_{Kpipe}}{z_{pipe} + z_{fluid} + z_{rad2}}\right), \tag{36}$$

where $z_{fluid} = -2\mathrm{i}B_f/a\omega$, $z_{pipe} = \mathrm{i}(\rho h\omega - Eh/a^2\omega)$, $z_{Kpipe} = -\mathrm{i}Eh/a^2\omega$ and $z_{rad2} = z_{d2} + z_{r2}$.

The magnitudes of the individual terms and their variation with frequency are considered in more detail in section 5, where example results are discussed.

(4) Returning to equation (33), if a surrounding medium is present, the radiation impedance terms contribute. The radiation mass and resistance terms are always both non-zero, thus k_2 is complex and the shell wave decays as it propagates along the pipe, radiating into the surrounding medium. The effect of the radiation mass is to increase the wavenumber k_2, thus reversing the effect of the contained fluid on the shell wave. If the shell wall material is lossy, equation (33) becomes

$$k_2^2 = k_L^2\left(1 + \frac{\nu^2}{1-\nu^2}\frac{Eh/a^2(1+i\eta)}{(Eh/a^2) + (2B_f/a) - \omega^2(\rho h + M_{rad}) + \mathrm{i}(\omega R_{rad} + \eta Eh/a^2)}\right). \tag{37}$$

As for the $s = 1$ wave, at low frequencies, the pipe wall loss dominates; at higher frequencies, radiation losses will dominate.

TABLE 1

Pipe properties

Thickness/radius ratio	0·125
Young's modulus (N/m^2)	$5{\cdot}0 \times 10^9$
Density (kg/m^3)	2000
Poisson's ratio	0·4
Material loss factor	0·065
Plate compressional wavespeed (m/s)	1725

TABLE 2

Media properties

	Surrounding medium	Contained fluid
Bulk modulus (N/m^2)	$4{\cdot}5 \times 10^9$	$2{\cdot}25 \times 10^9$
Shear modulus (N/m^2)	$1{\cdot}8 \times 10^8$	—
Density (kg/m^3)	2000	1000
Longitudinal wavespeed (m/s)	1500	1500
Shear wavespeed (m/s)	300	—

The above effects are discussed further in the following section where example results are shown.

5. EXAMPLE RESULTS

Example results are presented here for a typical water-filled PVC pipe surrounded by an infinite elastic medium which can sustain both longitudinal and shear waves. Results for the same water-filled pipe *in vacuo* are also shown for comparison. Complex wavenumbers for both the $s = 1$ and 2 waves are plotted as a function of frequency. Loss within the pipe wall is included, and is achieved by means of a complex modulus of elasticity, as discussed in the previous section. The various pipe and media properties are shown in Tables 1 and 2. Dispersion plots, derived by using equations (25) and (31) are shown in Figures 3, 4, 6 and 7. All the results are non-dimensionalized by the pipe radius, a, and plotted against the non-dimensional freefield fluid wavenumber $k_f a$. In addition, Figures 5 and 8 show the real and imaginary parts of the component impedances for each of the s waves.

Figure 3 shows the real part of the wavenumber for the $s = 1$ wave. Firstly, the figure shows that k_1 is much larger than the plate compressional wavenumber, k_L, consistent with the initial assumption about the $s = 1$ wave. The figure shows that, without the surrounding medium, the effect of the pipe wall compliance is to increase the real part of the wavenumber k_1 for the $s = 1$ wave from the freefield value, k_f: i.e., the wavespeed is reduced, as expected. The effect of the surrounding medium is to increase the wavenumber yet further, again as expected, given that the effect of the surrounding fluid is one of mass loading. This effect, however, is small compared with the effect of the shell wall, and certainly, at low frequencies, k_1 may be approximated by the *in vacuo* value, as expected. In this instance, k_1 is greater

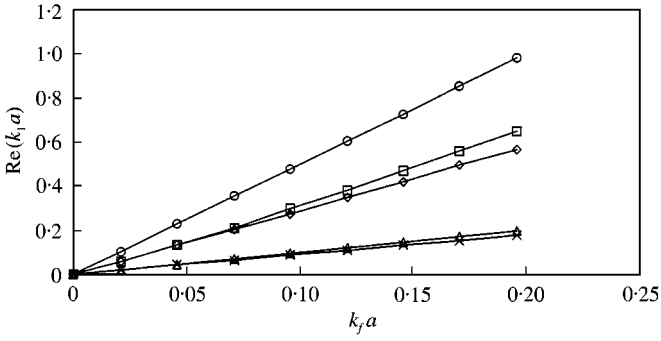

Figure 3. Real part of wavenumber for $s = 1$ wave: —◇—, fluid-filled *in vacuo* pipe; —□—, fluid-filled buried pipe; —△—, longitudinal wave, —△—, fluid wave; —○—, shear wave; —×—, plate wave.

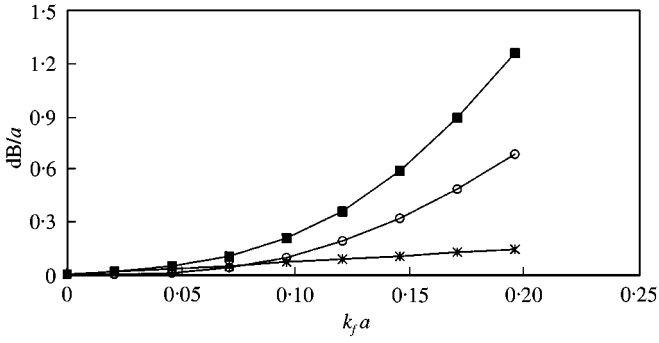

Figure 4. Loss in dB/unit distance for $s = 1$ wave: —✳—, material loss; —■—, total loss; —○—, shear wave loss.

than k_d and less than k_r (the wavespeed of the k_1 wave is greater than that of the shear wave in the surrounding medium, and less than that of the longitudinal wave), indicating that the shear wave radiates, whereas the longitudinal wave does not.

Figure 4 shows the loss in dB/unit propagation distance (measured in the number of pipe radii) for the $s = 1$ wave. This loss is related to the imaginary part of the wavenumber by

$$Loss \text{ (dB/unit distance)} = 20 \operatorname{Im}\{ka\}/\ln(10).$$

The approximate loss attributable to each mechanism is also shown. As the longitudinal wave does not radiate into the surrounding medium, no radiation losses are attributable to it; only the shear wave contributes to the radiation loss. It can be seen that the loss due to each mechanism increases with frequency. At low frequencies (approximately $k_fa < 0{\cdot}1$ on the graph), losses within the pipe wall dominate, whilst, at higher frequencies ($k_fa > 0{\cdot}1$ on the graph), the radiation resistance has increased sufficiently for the radiation loss to dominate.

Figure 5 shows the real and imaginary components of the fluid, pipe and radiation impedances for the $s = 1$ wave. Figure 5(a) shows that the radiation resistance increases with frequency as expected from equation (23). The real part of the pipe impedance decreases with frequency as expected—one of the consequences of adopting a frequency-independent loss factor. From Figure 5(b), it can be seen that the fluid and pipe impedances are stiffness-like (the frequencies considered are well below the pipe ring frequency), and the

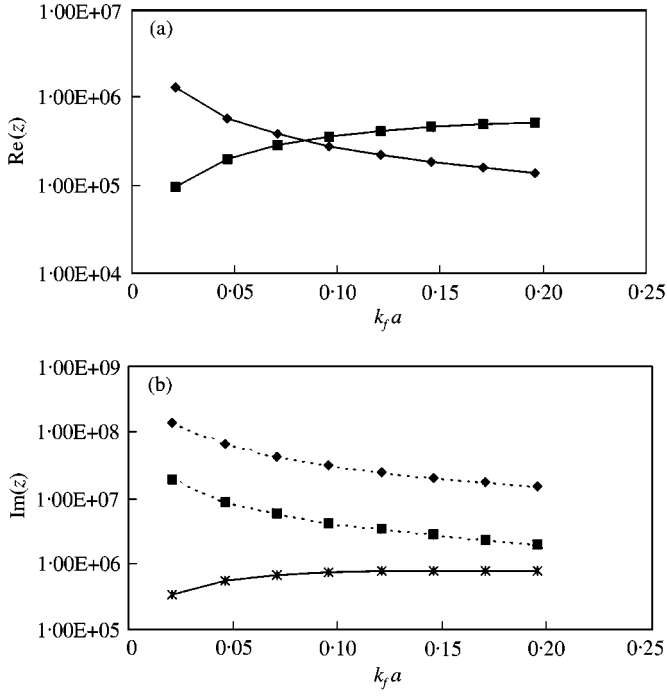

Figure 5. Component impedances for $s = 1$ wave: (a) real part: —◆—, pipe; —■—, radiation; (b) imaginary part: - -◆- -, fluid; - -■- -, pipe; —✳—, radiation (dotted lines indicate negative values).

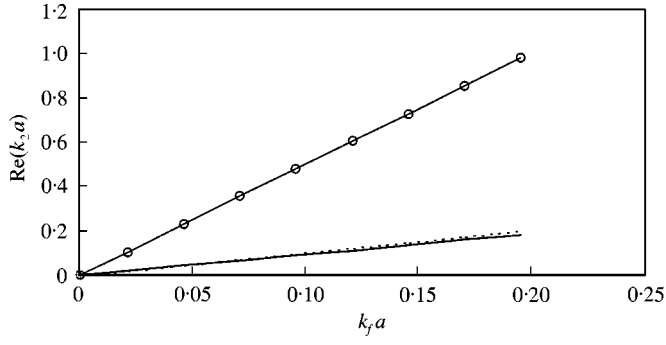

Figure 6. Real part of wavenumber for $s = 2$ wave: ——, fluid-filled *in vacuo* pipe; ——, fluid-filled buried pipe; -----, longitudinal wave; – – – – –, fluid wave; —○—, shear wave; ——, plate wave.

radiation impedance is mass-like, as expected. The ratio between the fluid impedance and pipe impedance is large, which, from examination of equation (28), is reflected in the observation that the presence of the pipe wall has a large effect on the $s = 1$ wavenumber. The magnitude of the radiation impedance is small compared with the pipe impedance, again reflected in the observation that the surrounding medium has a small effect on the $s = 1$ wave compared with the pipe wall itself. A close examination of equation (28) suggests that at any given frequency, the imaginary part of the $s = 1$ wavenumber will be controlled by whichever is the larger of the real parts of the pipe and radiation impedances. The results confirm this: Figures 4 and 5(a) show that when the real part of the pipe impedance is larger,

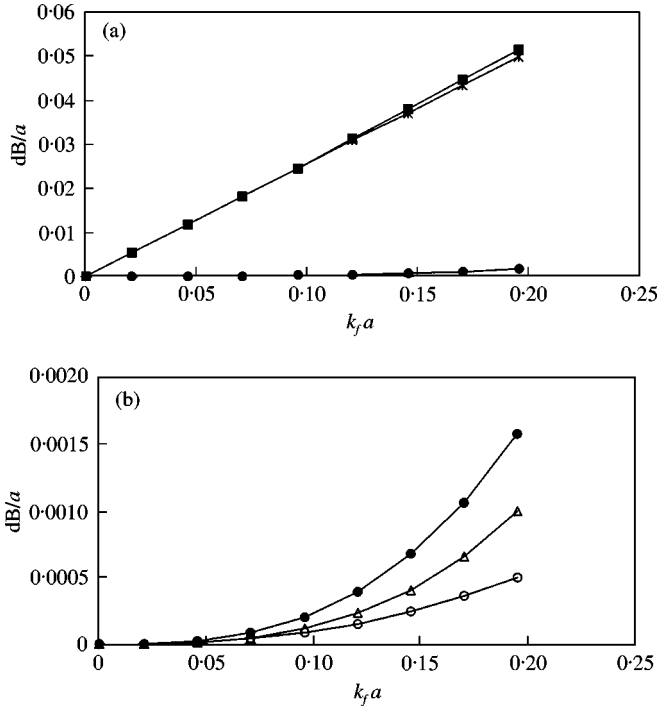

Figure 7. Loss in dB/unit distance for $s = 2$ wave: (a) all losses: —✳—, material loss; —■—, total loss; —●—, total radiation loss; (b) radiation loss: —○—, shear wave loss; —△—, longitudinal wave loss; —●—, total radiation loss.

the material loss dominates, and when the real part of the radiation impedance is larger, the radiation loss dominates.

Figure 6 depicts the real part of the $s = 2$ wavenumber, for both the fluid-filled pipe *in vacuo*, and with the surrounding medium. The graph shows that the wavenumber k_2 approximates to the plate compressional wavenumber k_L, and is not significantly affected by the presence of the surrounding medium. This is as expected given that the stiffness of the contained fluid is large compared with the pipe wall stiffness. The wavenumber k_2 is smaller than the wavenumbers for both the longitudinal and shear waves in the surrounding medium, so both the wave types will radiate. However, the wavenumber k_2 is not substantially smaller than the fluid wavenumber k_f, or the longitudinal wavenumber, k_d, as initially assumed, because the plate compressional wavenumber is comparable to the fluid and longitudinal wavenumbers. The effect of this is that the radial wavenumbers will be slightly smaller than predicted, and the radiation impedance will no longer be that of a pulsating cylinder. Examination of Figures 2(a) and 2(b) shows that, at low frequencies, the radiation resistance will be largely unaffected, but the radiation mass loading will be slightly larger than predicted. At higher frequencies, both the radiation resistance and the mass loading will be larger than predicted. The effect of this will be to reduce the wavespeed of the $s = 2$ wave somewhat, such that the wavenumber is likely to be slightly higher than that shown in the figure.

Figures 7(a) and 7(b) show the loss in dB/unit propagation distance (measured in number of pipe radii) for the $s = 2$ wave. The losses attributable to each mechanism separately are also shown. As for the $s = 1$ wave, losses increase with frequency for all the loss

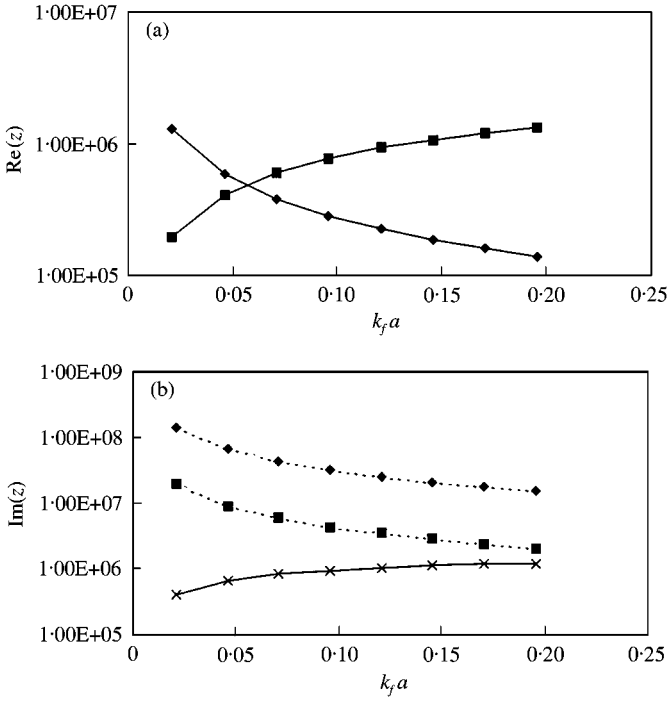

Figure 8. Component impedances for $s = 2$ wave: (a) real part: —◆—, pipe; —■—, radiation; (b) imaginary part: --◆--, fluid; --■--, pipe; —×—, radiation (dotted lines indicate negative values).

mechanisms. For all the frequencies shown, material losses dominate, showing that most of the energy loss for the $s = 2$ wave occurs in the pipe wall. Losses to the longitudinal wave are of a similar magnitude to those for the shear wave. This again is as expected, given that, at low frequencies, the radiation resistance for each wave (equation (23) is the same).

Figure 8 shows the real and imaginary components of the fluid, pipe and radiation impedances for the $s = 2$ wave. As for Figure 5(a), Figure 8(a) shows that the radiation resistance increases with frequency as expected whilst the real part of the pipe impedance decreases with frequency. From Figure 8(b), as expected, it can be seen that the fluid and pipe impedances are stiffness-like (the inertial term in the pipe impedance is small at the frequencies considered), and the radiation impedance is mass-like. Unlike for the $s = 1$ wave, there is no simple relationship between the relative sizes of the real parts of the pipe and radiation impedances and the controlling loss mechanism. However, an examination of equation (36), and its comparison with equation (28) (the magnitude of the radiation impedance is small compared with the pipe impedance, and even smaller compared with the fluid impedance) suggests that the effect of the surrounding medium is likely to be small. The wavenumber plots confirm this.

6. CONCLUSIONS

In this paper, axisymmetric waves in a fluid-filled, plastic pipe, surrounded by an infinite elastic medium which can sustain both longitudinal and shear waves have been studied.

Complex wavenumbers have been derived for two wave types: the $s = 1$ wave which is predominantly a fluid-borne wave; and the $s = 2$ wave which predominantly exists in the pipe wall. The real part of the wavenumbers provides information about the wavespeed of the wave, whilst the imaginary part relates to the propagation loss.

It was found that, for the "fluid-borne" $s = 1$ wave, the presence of the pipe wall reduces the wavespeed from the freefield value. The presence of the surrounding medium is to reduce it yet further, as it mass loads the pipe, but the effect is small compared with the effect of the pipe wall. The wave may or may not radiate into the external medium depending on its wavespeed relative to those in the surrounding medium. However, even if the wave does radiate, at low frequencies, losses within the shell wall will dominate.

For this $s = 2$ "shell" wave, the effect of both the contained fluid and the surrounding medium on the wavespeed is small. However, whereas the contained fluid is experienced as a stiffness by the pipe wall, thus slightly increasing the wavespeed, the surrounding medium is experienced as a mass, resulting in a slight reduction in wavespeed. The wave always radiates into the surrounding medium, but at all the frequencies considered, the radiation losses are small compared with the losses within the pipe wall.

ACKNOWLEDGMENT

The EPSRC are gratefully acknowledged for their support of this work.

REFERENCES

1. H. V. FUCHS and R. RIEHLE 1991 *Applied Acoustics* **33**, 1–19. Ten years of experience with leak detection by acoustic signal analysis.
2. O. HUNAIDI and W. T. CHU 1999 *Applied Acoustics* **58**, 235–254. Acoustical characteristics of leak signals in water distribution pipes.
3. S. MARKUS *The Mechanics of Vibrations of Cylindrical Shells*: *Studies in Applied Mechanics*, Vol. 17. Amsterdam: Elsevier.
4. M. C. JUNGER and D. FEIT 1986 *Sound*, *Structures*, *and Their Interaction*. Cambridge, MA: MIT Press.
5. R. J. PINNINGTON and A. R. BRISCOE 1994 *Journal of Sound and Vibration* **173**, 503–516. Externally applied sensor for axisymmetric waves in a fluid filled pipe. doi: 10.1006/jsvi.1994.1243.
6. C. R. FULLER and F. J. FAHY 1982 *Journal of Sound and Vibration* **81**, 501–518. Characteristics of wave propagation and energy distributions in cylindrical elastic shells filled with fluid.
7. M. L. MUNJAL and P. T. THAWANI 1996 *Journal of Noise Control Engineering* **44**, 274–280. Acoustic performance of hoses—a parametric study.
8. M. C. JUNGER 1953 *The Journal of the Acoustical Society of America* **25**, 40–47. The physical interpretation of the expression for an outgoing wave in cylindrical coordinates.
9. M. J. S. LOWE 1995 *IEEE Transactions on Ultrasonics*, *Ferroelectrics and Frequency Control* **42**, 525–541. Matrix techniques for modelling ultrasonic waves in multilayered media.
10. C. ARISTÉGUI, P. CAWLEY and M. LOWE 1999 *Review of Progress on Quantitative Nondestructive Evaluation* (D. O. Thompson and D. E. Chimenti, editors), Vol. 18. Dordrecht/New York: Kluwer Academic/Plenum Publishers. Guided waves in fluid filled pipes surrounded by different fluids: prediction and measurement.
11. E. H. KENNARD 1953 *Journal of Applied Mechanics*, 33–40. The new approach to shell theory: circular cylinders.
12. M. ABRAMOWITZ and I. A. STEGUN 1965 *Handbook of Mathematical Functions*. New York: Dover publications.
13. B. PAVLAKOVIC 1998 *Ph.D. Thesis*, *London University*. Leaky guided ultrasonic waves in NDT.
14. D. I. KORTEWEG 1878 *Annalon der Physik* **5**. Uber die fortpflanzungsgeschwindigkeit des schalles in elastischen röher (On the speed of sound in water in flexible pipes).

APPENDIX A: NOMENCLATURE

x, θ, r	axial, circumferential and radial directions
u, v, w	shell displacements in the axial, circumferential and radial directions
σ_x, σ_θ	axial and circumferential normal stress
a, h	pipe radius, wall thickness
p_f, p_m	pressures in the contained and surrounding media
ρ, E, v	density, elastic modulus, Poisson ratio of shell material
U_s, W_s	amplitudes of axial and radial displacements of the s wave
P_{fs}, P_{ds}, P_{rs}	pressure amplitudes of the s wave in the contained and surrounding media
k	wavenumber
k_s	axial wavenumber of the s wave
k_f	freefield internal fluid wavenumber
k_d, k_r	freefield wavenumber of longitudinal and shear waves in the surrounding medium
k_L	axial wavenumber of a compressional wave in a plate of the shell thickness
k^r_{fs}, k^r_{ds}, k^r_{rs}	radial wavenumber for the s wave in the contained and surrounding media
B_f, B_m	bulk moduli of the contained and surrounding media
ρ, G_m	density, shear modulus of the surrounding medium
z_{ds}, z_{rs}	radiation impedances of the s wave in the surrounding medium
c_d, c_r	wavespeeds of longitudinal and shear waves in the surrounding medium
M_{rad}, R_{rad}	radiation mass, resistance